Chapter - 3

Hydrodynamics Using Non-Newtonian Liquids

This chapter deals with the experimental investigation using air–non-Newtonian liquids in batch. The gas holdup and pressure drop in tapered bubble columns have been reported in this chapter. The effects of different operating variables such as liquid flow rate, bed height, orifice diameter of sieve plate, etc. on gas holdup and frictional pressure drop have been investigated. Empirical correlations have been developed to predict the gas holdup and frictional pressure drop.

3.1 Introduction

A large number of studies have been reported in literature on the measurement and analysis of gas hold up and pressure drop in gas-Newtonian liquid flow systems. Various models and correlations have also been proposed. In the field of biotechnology, chemical, petrochemical, polymer and pharmaceutical industries the liquid used are often non-Newtonian in nature. In fermentation process initially liquid is Newtonian and then gradually it is converted to non-Newtonian. Bubbles in non-Newtonian liquid behaves as various shapes and under the action of surface tension, inertia force, viscous drag force and buoyancy, together with the complex rheological behaviour of the liquids and hence the bubble flows in these liquids has different characteristics than that of Newtonian liquids (Chhabra,1988). Bubble behaviour (i.e. formation, rising, coalescence, splitting) in these liquids affects the performances in various process application like polymer devolatilisation, composite processing, fermentation, organic synthesis, plastic foam processing, etc. (Olivieri et al., 2011). The theoretical and experimental studies on bubble flow in non-Newtonian liquids have been reviewed by Chhabra (2007). Only few literatures are available using non-Newtonian liquid in bubble column (Godbole et al., 1982; Schumpe and Deckwer, 1982; Haque et al., 1986; Li, 1999; Pradhan et al., 1993; Lakota, 2007; Anastasiou et al., 2013).

Chandrakar (1985) reported a detailed experimental analysis of gas-non-Newtonian in upflow bubble column with ejector type gas distributor. Lakota (2007) studied the upflow bubble column using non-Newtonian liquids with concurrent upflow mode, also liquid batch mode and developed empirical correlation for holdup prediction for each case. Das et al. (1992) developed empirical correlation for gas-non-Newtonian liquid upflow in vertical column. They also developed empirical correlation for frictional pressure drop prediction (1995). Pradhan et al. (1993) studied the effects of internals in the bubble column using non-Newtonian pseudoplastic liquids. Mandal et al. (2003) studied gas entrainment and holdup characteristics in down flow bubble column with both Newtonian and non-Newtonian liquid and later they also reported the frictional pressure drop (2004). Jawad (2009) exclusive study pressure drop characteristics in bubble column using SCMC solution. Chandarkar et al. (2009) reported that the gas dispersion in non-Newtonian liquid in a co-current vertically up flow bubble column. Liquid circulation induced by the bubble movement is important phenomena observed in gas bubbling in viscous liquids and is reviewed by Haque et al. (1987). Anastasiou et al. (2013) developed an empirical correlation to predict the gas holdup for shear thinning non-Newtonian liquid in bubble columns with a metal porous sparger to provide very fine air bubbles. In the present study tapper bubble columns are fabricated to study its hydrodynamic characteristics using non-Newtonian pseudo plastic liquids. The knowledge of pressure drop also gives the energy losses and it helps in modeling of such system. But effect of bubble formation and form drag due to interaction of bubbles on pressure drop in tapered bubble column has not yet been reported. In view of the importance of non-Newtonian liquids and the advantages accessible by tapered bubble column, the present work has been undertaken for the study of non-Newtonian liquid in batch bubble columns.

3.2 Experimental Procedure

The liquid was charged into the column batch wise. The liquid heights used for the experiments were 1.12 m, 1.17 m and 1.22 m for both columns. The air at a pressure $1 kg/cm^2$ gauge was introduced into the columns, and under steady state condition, reading of manometers attached to the tapings were noted and also the height of liquid column was noted. The experiment was performed in a semi-continuous manner i.e. batch with respect to the liquid phase and continuous with respect to gas phase. Manometers would be attached to the tapings, which would be located at different heights in the column. From the manometer readings pressure drop will be determined. Flow pattern was observed visually and it was bubble and plug according to the increasing air flow rate. The experiments were repeated a number of times to ensure the reproducibility of the data. The temperature was maintained at atmospheric temperature30 ± 2^0C.

3.3 Results and discussion

3.3.1 Effective Shear rate

In the case of non-Newtonian liquids the viscosity is a function of shear rate and it is generally expressed as effective viscosity, μ_{eff}. To estimate the effective viscosity, the effective shear rate, $\dot{\gamma}_{eff}$, in the bubble column has to be calculated first. For the Power law model the effective viscosity is defined as

$$\mu_{eff} = K\dot{\gamma}_{eff}^{n-1} \qquad (3.1)$$

Literature review suggested that $\dot{\gamma}_{eff}$ is proportional to the superficial gas velocity as the shear originates from the relative velocity between bubbles and the liquid in the bubble column and expressed as (Schumpe and Deckwer, 1987; Nishikawa et al., 1977; Henzler, 1984),

$$\dot{\gamma}_{eff} = Cu_g \tag{3.2}$$

The constant, *C*, value suggested by different researchers are as follows,

Nishikawa et al. (1977)	$C = 5000\ m^{-1}$ for *n* varies from 1 to 0.72
Henzler (1984)	$C = 1500\ m^{-1}$ for *n* varies from 0.82 to 0.38
Schumpe and Deckwer (1987)	$C = 2800\ m^{-1}$ for *n* varies from 1 to 0.180

Nishikawa et al. (1977) obtained the value of *C* by fitting the heat transfer coefficient data measured in Newtonian and non-Newtonian system. Henzier (1984) obtained the *C* value by fitting mass transfer coefficient data in non-Newtonian liquids in a bubble column tower reactor. Schumpe and Deckwer (1987) proposed the value of *C* for their studied in tower reactors for different diameter and using different viscous liquid. The applicability of the Nishikawa et al. (1977) and Henzier (1984) correlation was in questioned by number of researchers (Allen et al., 1991; Chisti et al., 1989; Kawase et al., 1991 and Al-Masry, 1999). In present study, *C* is taken as 2800 m^{-1} and effective viscosity was measured by using Eq. (3.2) Schumpe and Deckwer (1987).

3.3.2 Bubble characteristics and flow regime

At very low air flow rate the bubbles of equal size are forms which demonstrate homogeneous flow region, but it's exist only for small range of flow rate variation. As, the air flow rate increases, strong convective motion result which brings the bubble close together allowing coalescence leading to the formation of larger bubbles. When the bubbles are sufficiently large and the concentration of SCMC solution is high enough, the bubble appear to be cups at its lower end. Similar results are also observed by other researchers (Hassager, 1979; Malaga and Rallison 2007). These large bubbles rises in the centre of the column, carrying considerable amount of liquid and many small bubbles in their wake. Once the large bubbles reach the liquid surface, the small bubble in the wake are entrained by the liquid down flow and are swept downward at the sides of the column. Almost entire range of the study the flow pattern was heterogeneous as bubbles of varying size were produced. The flow pattern in the tapered bubble column consists of two zones, central zone and annular region. In the central zone most of the bubble rises and whereas the bubble breakup and downward flow occurs in the annular region (Hassager, 1979; Sen, 2003). At high gas flow rate the bubbles burst at the surface causing ejection of fines of liquid droplets and inward dipping in the annular region (Fig. 3.1). Fig. 3.2 shows that the static pressure at 3rd or 4th manometer tapping suddenly increases and is due to re-entered of the gas-liquid flow from the annular region to main central region.

It was observed that the bubbles expanded spherically at close to the orifice plate and evolved from the spherical shape to teardrop shape as it passes upwards. Initially the surface tension is dominated near the orifice plate and hence the bubbles are spherical in shape and as it flows upward the buoyancy plays an important role in the growth of bubble and also coalescence takes place. As bubbles move upward they tend to be elongated in shape and then in teardrop shape. As the bubbles move upward the non-Newtonian liquid is stretched because the reduction of viscosity takes place. In the shear thinning non-Newtonian liquid the apparent viscosity around the bubble decreases due to shear hence bubble can raise more easily. The viscosity of the liquid around the bubble varies; it depends on the shape of the bubble and shear-thinning property of the liquid, and the decrease of viscosity is more in the close vicinity of the bubble. The high viscosity region exists in the wake of these bubbles. The bubble rise velocity increases gradually due the strong shear-thinning effect. As shear-thinning effect becomes intensive the bubble takes the more oblate shape with the front surface flatter than the rear part (Malage and Rallison, 2007). Similar observation is also reported by Anastasiou et al. (2013) and Fransolet et al. (2005). Vélez-Cordero and Zenit (2011) also identify the possibility of bubble cluster formation below the property group (N_{pl}) value of 1 X 10^{-3}.

3.3.3 Frictional pressure drop

The pressure drop in the vertical flow is the sum of the frictional pressure (ΔP_f), the hydrostatic head component (ΔP_h) and pressure drop due to accelerative effects (ΔP_a). Thus,

$$\Delta P_T = \Delta P_f + \Delta P_h + \Delta P_a \tag{3.3}$$

According to Hughmark and Pressburg (1961) and Friedel (1980) acceleration component (ΔP_a) is insignificant compared to the total pressure drop. Hence,

$$\Delta P_T = \Delta P_f + \Delta P_h \tag{3.4}$$

Many researchers, Ros, 1961; Hagedron and Brown, 1965; Mondal et al., 2004, have considered the in-situ density of the two-phase system for the calculation of the hydrostatic head by assuming the overall gas holdup in the column is same everywhere,

$$\Delta P_h = g\Delta Z\left(\rho_l \varepsilon_l + \rho_g \varepsilon_g\right) \tag{3.5}$$

As $\rho_l >> \rho_g$ the second term within the bracket of the right hand side can be neglected.

Thus substituting ΔP_h from Eq. (3.5) in Eq. (3.4), one gets

$$\Delta P_T = \Delta P_f + g\Delta Z \rho_l \varepsilon_l \tag{3.6}$$

Therefore,

$$\Delta P_f = \Delta P_T - g\Delta Z \rho_l \varepsilon_l \tag{3.7}$$

or,

$$\frac{\Delta P_f}{\rho_l g \Delta Z} = \frac{\Delta P_T}{\rho_l g \Delta Z} - \varepsilon_l \tag{3.8}$$

Hence,

$$\Delta P = \frac{\Delta P_T}{\rho_l g \Delta Z} - \varepsilon_l \tag{3.9}$$

In present study frictional pressure drop (ΔP) calculated from Eq. (3.9).

3.3.4 Effect of SCMC Concentration

Fig. 3.3 shows the variation of gas holdup with gas flow rate at different constant bed heights (1.22 m, 1.17 m, 1.12 m) for SCMC solutions. It is clear that the gas holdup increases with increasing gas flow rate at different constant bed height. As bed height increases the gas holdup decreases with increasing gas flow rate. This is due to bubble coalescence in the column and its rise velocity increases Wallis (1969) and Voigt et al. (1979). Fig. 3.4 shows the variation of gas holdup with gas flow rate at different SCMC concentrations. The gas holdup decreases with increasing SCMC concentration at constant gas flow rate. With increasing SCMC concentration effective viscosity increases, at higher SCMC concentration the dense medium will tend to reduce the bubble rise velocity and led to longer residence time and also coalescence the bubbles due to decrease of turbulence in the liquid phase and it favors the formation of larger sized bubbles which increase the bubble rise velocity. As SCMC concentration increases the density of the solution increases it leads to increase in buoyancy and hence bubble raises velocity. In these two opposite effects the latter is more predominant and is responsible for the low gas holdup at higher SCMC concentration. With the increase in SCMC concentration the surface tension increases the expansion of bubble surface is difficult and the bubble volume increases with coalescence only in the column. Similar results are also reported by other researchers (Chhabra, 1988; Chhabra, 2007; Li, 1999; Chandarkar et al., 2009; Malaga and Rallison, 2007).

Fig. 3.5 shows the variation frictional pressure drop with gas flow rate at different bed heights. It is clear from the figure that the frictional pressure drop increases with increasing gas flow as bed height increases the frictional pressure drop also increases with increasing gas flow rate. Because larger bed height and the residence time of the bubbles is increased this leads to larger frictional pressure. Fig. 3.6 shows the variation of frictional pressure drop with gas flow rate at different SCMC concentrations. It is clear from the figure that the frictional pressure drop increases with increasing the gas flow rate for different SCMC solutions and with increasing SCMC concentration the frictional pressure drop increases with gas flow rate. The effective viscosity increase with increasing SCMC concentration and it leads to increase frictional pressure drop in the column as gas flow rate is increased. This is due to at higher concentration, dense medium will tend to suppress and coalescence the bubbles, hence increases frictional pressure drop.

3.3.5 Effect of orifice diameter

Bubble detachment volume gradually increases with the increase in orifice diameter, so the bubble size increases with the orifice diameter. It was observed that the volume of the bubbles changes very sharply with the change in orifice diameter. Both the drag force and surface tension increase with the orifice diameter, and these forces prevent the bubble detaching quickly from orifice. Hence, the bubble growth become larger and bubble volume increases. Fig. 3.7 shows the variation of gas holdup with gas flow rate at different distributor hole diameters. It is clear that as the distributor hole diameter increases the gas holdup decreases due to bigger sized bubble generation with higher bubble rise velocity. Fig. 3.8 shows the variation of frictional pressure drop with gas flow rate at different distributor hole diameter. It is clear that frictional pressure drop increases with gas flow rate at different distributor hole diameters. As distributor hole diameter increases frictional pressure drop increases due to the formation of bigger sized bubbles.

3.3.6 Effect of taper angle

Figs. 3.9 – 3.10 show the effect of taper angle on the gas holdup and frictional pressure drop respectively. It is clear from the figures that as the taper angle decrease the gas holdup and frictional pressure drop increases. At lower taper angle back mixing is more and at higher taper angle the liquid at near the wall in the top portion of the column is remain unaffected. i.e., stagnant and hence gas holdup and pressure drop decreases. Increasing the taper angle the cross sectional area particularly in the upper zone increases which minimizes the transition of flow pattern and also reduce the coalescence. In the case small taper angled bubble column the coalescence of bubbles are more, large sized bubble having higher rise velocity and followed by small sized bubbles. Few of these small sized bubbles are recirculated through the annular region and are responsible for higher gas holdup and frictional pressure drop. Whereas for higher taper angled bubble column the rate of recirculation is low due higher cross-sectional area in the upper zone and some portion close to the wall in the upper half of the column remain unaffected by the bubble.

3.3.7 Comparison with literature

Several empirical correlations for gas holdup are available in literature. Schumpe and Deckwer (1982) suggested the following correlation for their experiment in 0.102 m diameter bubble column using air-CMC solution in churn-turbulent flow regime,

$$\varepsilon_g = 0.725 U_g^{0.627} \tag{3.10}$$

This correlation does not take into account the physical properties of the system. Godbole et al. (1982) developed the following correlation for churn-turbulent flow regime

$$\varepsilon_g = 0.225 U_g^{0.532} \mu_{eff}^{-0.146} \text{ for } U_g \geq 0.03 \text{ m/s and } 0.10 \text{ m} \leq D_c \leq 1.0 \text{ m} \tag{3.11}$$

Vatai and Tekic (1987) reported the experimental investigation of gas holdup using non-Newtonian liquids and presented the following empirical correlation,

$$\varepsilon_g = 0.95 \left(\frac{U_g \mu_{eff}}{\sigma_l}\right)^{0.769} \left(\frac{\mu_{eff}^4 g}{\rho_l \sigma_l^3}\right)^{-0.17} \left(\frac{\rho_g}{\rho_l}\right)^{0.062} \left(\frac{\mu_g}{\mu_{eff}}\right)^{0.107} \text{ for } D_c = 0.1\text{m}; H_o = 200 \text{ cm} \tag{3.12}$$

Fransolet et al. (2005) studied the effect of rheological behaviour of the non-Newtonian pseudoplastic liquids on gas holdup and flow pattern in a bubble column reactor and developed the following equation,

$$\varepsilon_g = 0.26 U_g^{0.54} \mu_{eff}^{-0.147} \text{ for } D_c = 0.24 \text{ m}, U_g \leq 0.15 \text{ m/s} \tag{3.13}$$

Lakota (2007) developed the following empirical correlation,

$$\varepsilon_g = 0.0524 U_g^{0.623} \mu_{eff}^{-0.0531} \text{ for } 0.018 m/s \geq U_g \geq 0.252 m/s \text{, and } D_c\text{=2.62 m}$$

$$\text{and } H_o = 2.37 \text{ m} \tag{3.14}$$

Except Eq. (3.12) all these correlations only viscosity term have been introduced, the effect of other physical properties and system variables have not been consider. In Eq. (3.12) the system variables are not consider.

Jawad (2009) proposed the following empirical correlation in heterogeneous churn turbulent flow regimes.

$$\Delta P = 16108 n^{0.16} \mathrm{Re}_g^{-0.0398n} Fr_g^{0.037n} \tag{3.15}$$

Where, the unit of ΔP is Pa. The experimental gas holdup and total pressure drop is compared with the above equations and Tables 3.1-3.2 show the Relative error (RE) and Absolute error (AE). The Relative error and Absolute error are defined as,

$$RE = \frac{1}{N}\sum_{1}^{N}\left|\left(\frac{\varepsilon_{g\,\mathrm{expt}} - \varepsilon_{g\,cal}}{\varepsilon_{g\,\mathrm{expt}}}\right)\right| \times 100 \tag{3.16}$$

$$AE = \frac{1}{N}\sum_{1}^{N}\left|\left(\varepsilon_{g\,\mathrm{expt}} - \varepsilon_{g\,cal}\right)\right| \tag{3.17}$$

Godbole et al., 1982; Vatai and Tekic, 1987 and Fransolet et al., 2005 correlations are valid for very high gas flow rate and churn-turbulent flow regime. Lakota (2007) correlation is within our experimental range and Fig. 3.11 shows the comparison. Fig. 3.12 shows the comparison with the correlation available in the literature for total pressure drop. It clearly shows that the performance of the taper column is more effective than the conventional cylindrical column. As the above correlations are not correlate the experimental data, hence, in the present case a correlation has been developed by dimensional analysis to predict the gas holdup and frictional pressure drop as a function of the physical properties, geometric and dynamic variables of the system.

3.3.8 Empirical correlation

3.3.8.1 Correlation for the gas holdup

It is extremely difficult to approach a theoretical analysis of a completed system where bubble separation, coalescence and breakup, momentum transfer between the two phases, the wall friction, the shear at phase interface cannot be determined quantitatively Friedel (1980). Hence, in the present case a correlation is developed by dimensional analyses to predict the gas holdup and the frictional hydrodynamic parameters are the physical properties, geometric and dynamic variables of the system. The parameters affect the gas holdup for tapered bubble columns using non-Newtonian liquids are

(1) Physical properties of the gas and the liquid, namely, density ρ_g and ρ_l; viscosity μ_g and μ_{eff}; surface tension σ_l.

(2) Gas flow rate of the gas, Q_g.

(3) Diameter of the column and Distributor hole diameter, namely, D_c and D_n.

(4) Height of initial liquid in column, H_0.

(5) Taper angle (dimensionless), θ.

(6) Other parameter like acceleration due to gravity, g.

The gas holdup may be written as a function of all these variables as,

$$\varepsilon_g = F(Q_g, \mu_g, \rho_g, \rho_l, \mu_{eff}, \sigma_l, H_0, D_c, D_n, \theta, g) \tag{3.18}$$

The diameter of the column was calculated by calculating the equivalent diameter of the base and at the gas-liquid interface, then calculates the log mean diameter for the column,

D_c. Hence, for each gas flow rate the column diameter, D_c, varies according to the height of the gas-liquid interface.

Applying the Buckingham's π-theorem of dimensional analysis, gas holdup can be expressed by the following functional relationship with the various dimensionless groups.

$$\varepsilon_g = F\left(\frac{Q_g\rho_g}{\mu_g D_c}\right)\left(\frac{\rho_l}{\rho_g}\right)\left(\frac{\mu_{eff}}{\mu_g}\right)\left(\frac{\sigma_l\rho_g D_c}{\mu_g^2}\right)\left(\frac{H_0}{D_c}\right)\left(\frac{D_n}{D_c}\right)\left(\frac{g\rho_g^2 D_c^3}{\mu_g^2}\right)(\theta) \tag{3.19}$$

Combining some of these groups, one may obtains,

$$\frac{Q_g\rho_g}{\mu_g D_c} = \frac{M_g}{\mu_g D_c} = \mathrm{Re}_g \tag{3.20}$$

$$\left(\frac{\sigma_l\rho_g D_c}{\mu_g^2}\right)\left(\frac{\rho_l}{\rho_g}\right)\left(\frac{\mu_g}{\mu_{eff}}\right)^2 = \frac{\sigma_l\rho_l D_c}{\mu_{eff}^2} \tag{3.21}$$

$$\left(\frac{g\rho_g^2 D_c^3}{\mu_g^2}\right)\left(\frac{\rho_l}{\rho_g}\right)^2\left(\frac{\mu_g}{\mu_{eff}}\right)^2 = \frac{\rho_l^2 D_c^3 g}{\mu_{eff}^2} \tag{3.22}$$

$$\left(\frac{\rho_l^2 D_c^3 g}{\mu_{eff}^2}\right)\left(\frac{\mu_{eff}^2}{\sigma_l\rho_l D_c}\right)^3 = \frac{\mu_{eff}^4 g}{\rho_l\sigma_l^3} = N_{pl} \tag{3.23}$$

The functional relationship between gas holdup and the relevant physical, dynamic and geometric parameters can reduced to an equivalent functional relationship as,

$$\varepsilon_g = F\left(\mathrm{Re}_g, N_{pl}, \frac{H_0}{D_C}, \frac{D_n}{D_c}, \theta\right) \tag{3.24}$$

On the basis of Eq. (3.24), the multiple linear regression analysis of the experimental data yielded the following correlation,

$$\varepsilon_g = 3.857X10^{-4}\,\mathrm{Re}_g^{0.743\pm0.017}\,N_{pl}^{-0.009\pm0.003}\left(\frac{H_0}{D_C}\right)^{-0.565\pm0.038}\left(\frac{D_n}{D_C}\right)^{0.149\pm0.063}\theta^{-0.706\pm0.028} \tag{3.25}$$

for

$$6.0615 \le \mathrm{Re}_g \le 417.91$$
$$8.17\times10^{-8} \le N_{pl} \le 3.10\times10^{-2}$$
$$16.91 \le \left(\frac{H_0}{D_c}\right) \le 20.13$$
$$0.03914 \le \left(\frac{D_n}{D_c}\right) \le 0.07275$$
$$0.0077 \le \theta \le 0.015$$

where the liquid property group, $N_{pl} = \frac{\mu_{eff}^4 g}{\rho_l \sigma_l^3}$, signifies some complex balance between viscous, surface tension and gravitational force. The predicted values by the Eq. (3.25) have been plotted against the experimental values as shown in Fig. 3.13. The variance of the estimate and correlation coefficient of the above equation are 0.02191 and 0.9616 respectively for a t value of 1.98 for 641 degrees of freedom at 0.05 probability level and 95% confidence range Volk (1958).

3.3.8.2 Correlation for the frictional pressure drop

Similarly, the pressure drop may be written as a function of the following variables as,

$$\frac{\Delta P_f}{\rho_l g \Delta Z} = F(Q_g, \mu_g, \rho_g, \rho_l, \mu_{eff}, \sigma_l, H_0, D_c, D_n, \theta, g) \tag{3.26}$$

Applying the Buckingham's π-theorem of dimensional analysis, gas holdup can be expressed by the following functional relationship with the various dimensionless groups.

$$\frac{\Delta P_f}{\rho_l g \Delta Z} = F(\frac{Q_g \rho_g}{\mu_g D_c})(\frac{\rho_l}{\rho_g})(\frac{\mu_{eff}}{\mu_g})(\frac{\sigma_l \rho_g D_c}{\mu_g^2})(\frac{H_0}{D_c})(\frac{D_n}{D_c})(\frac{g \rho_g^2 D_c^3}{\mu_g^2})(\theta) \tag{3.27}$$

This functional relationship can be reduced to an equivalent functional relationship by combining some of these groups as,

$$\frac{\Delta P_f}{\rho_l g \Delta Z} = F(\mathrm{Re}_g, N_{pl}, \frac{H_0}{D_C}, \frac{D_n}{D_c}, \theta) \tag{3.28}$$

On the basis of Eq. (3.28), the multiple linear regression analysis of the experimental data yielded the following correlation,

$$\frac{\Delta P_f}{\rho_l g \Delta Z} = 8.071X10^{-4}\,\mathrm{Re}_g^{0.890\pm0.018}\,N_{pl}^{0.009\pm0.003}(\frac{H_0}{D_C})^{-0.350\pm0.040}(\frac{D_n}{D_C})^{0.209\pm0.067}\theta^{-0.381\pm0.030} \tag{3.29}$$

for

$$6.0615 \le \mathrm{Re}_g \le 417.91$$
$$8.17\times10^{-8} \le N_{pl} \le 3.10\times10^{-2}$$
$$16.91 \le \left(\frac{H_0}{D_c}\right) \le 20.13$$
$$0.03914 \le \left(\frac{D_n}{D_c}\right) \le 0.07275$$
$$0.0077 \le \theta \le 0.015$$

The predicted values by the Eq. (3.29) have been plotted against the experimental values as shown in Fig. 3.14. The variance of the estimate and correlation coefficient of the above equation are 0.02472 and 0.9685 respectively for a t value of 1.98 for 640 degrees of freedom at 0.05 probability level and 95% confidence range Volk (1958).

3.1.4 Conclusions

The gas holdup and frictional pressure drop have been measured in two different tapered bubble columns using non-Newtonian liquids. The gas holdup is higher for lower bed height. The gas holdup increases with lowering the pseudo plasticity of SCMC solution. The gas hold up increases with decreases the distributor hole diameter. The frictional pressure drop is higher for higher bed height. The frictional pressure drop increases with increasing the pseudo plasticity of SCMC solutions. The frictional pressure drop increases with an increase in the distributor hole diameter. Empirical correlations have been developed to calculate the gas holdup and frictional pressure drop as a function of various measurable parameters.

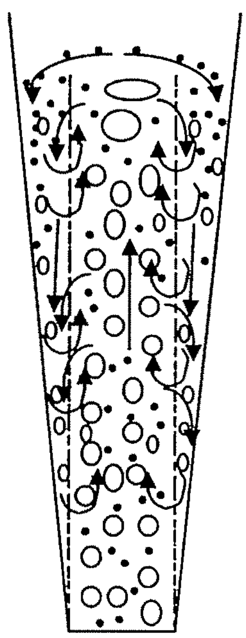

Fig. 3.1 Schematic diagram of the structure of a tapered bubble column

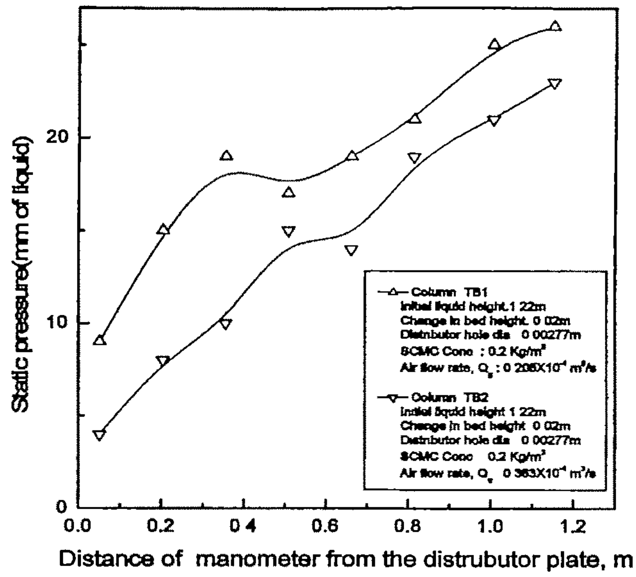

Fig. 3.2 Variation of static pressure with distance of manometer from the distributor Plate

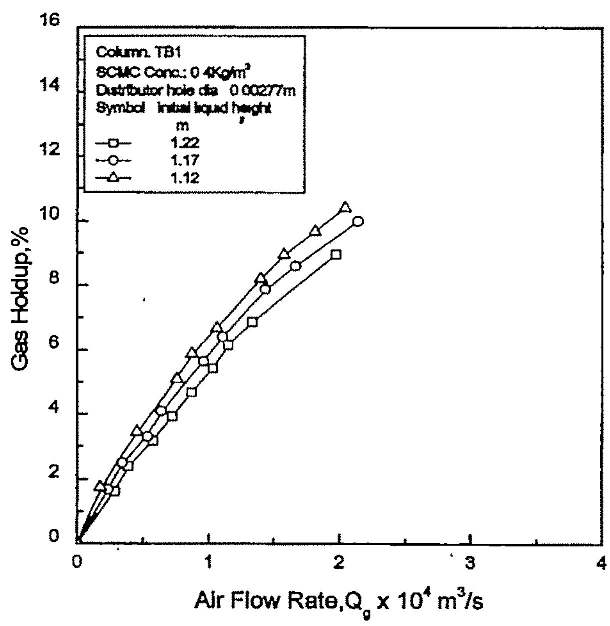

Fig. 3.3 Variation of gas holdup with gas flow rate at different clear liquid height

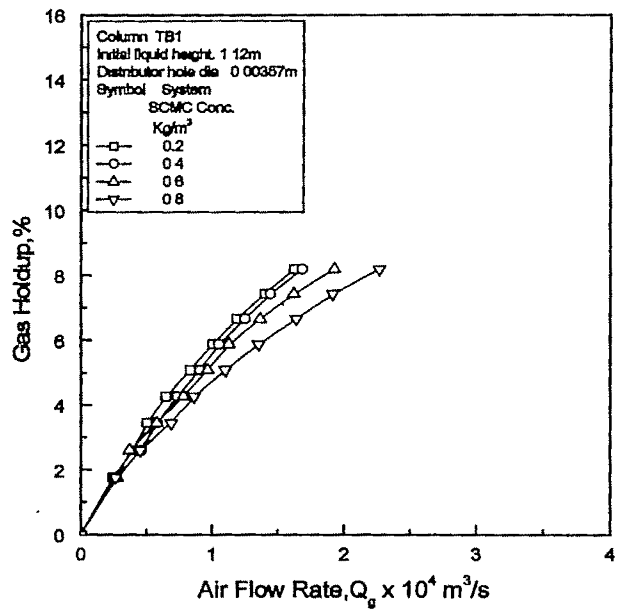

Fig. 3.4 Variation of gas holdup with gas flow rate at different SCMC solution concentration

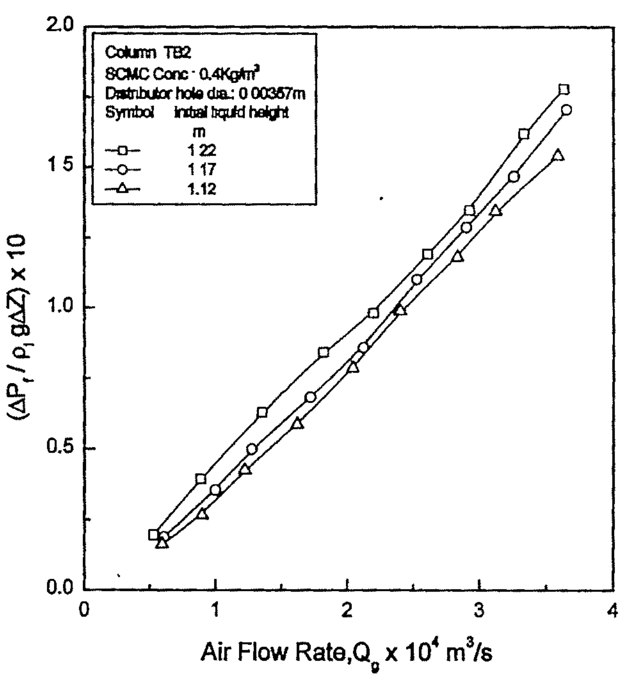

Fig. 3.5 Variation of frictional pressure drop with gas flow at different clear liquid height

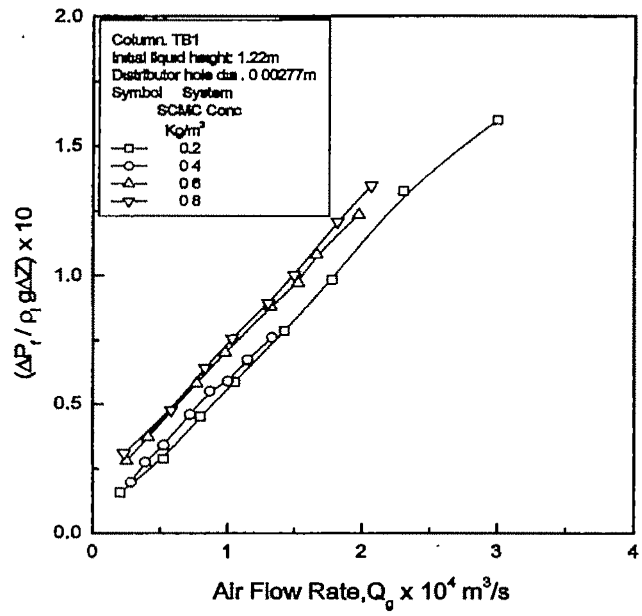

Fig. 3.6 Variation of frictional pressure drop with gas flow rate at different SCMC solution concentration

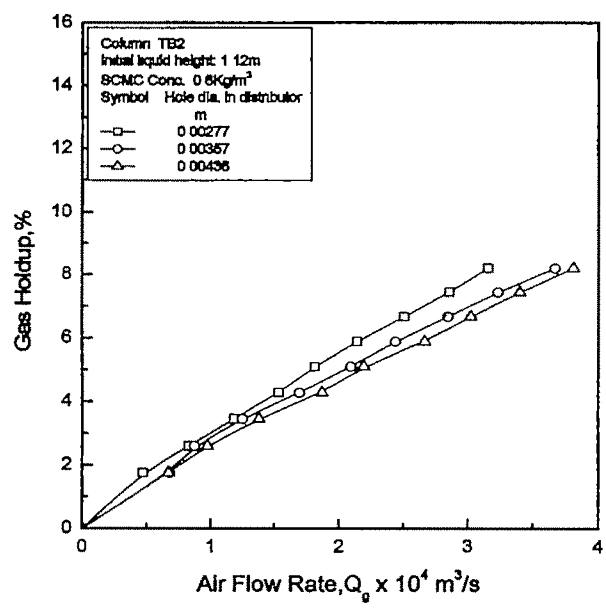

Fig. 3.7 Variation of gas holdup with gas flow rate at different hole diameter of the gas distributor

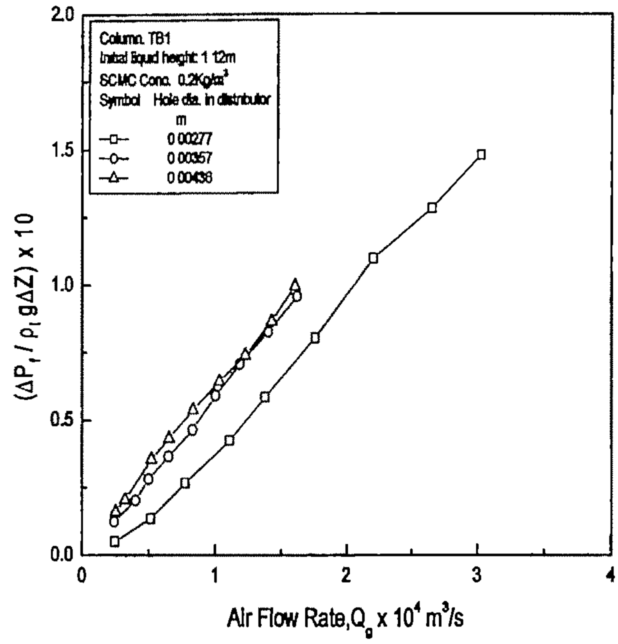

Fig. 3.8 Variation of frictional pressure drop with gas flow rate at different hole diameter of the gas distributor

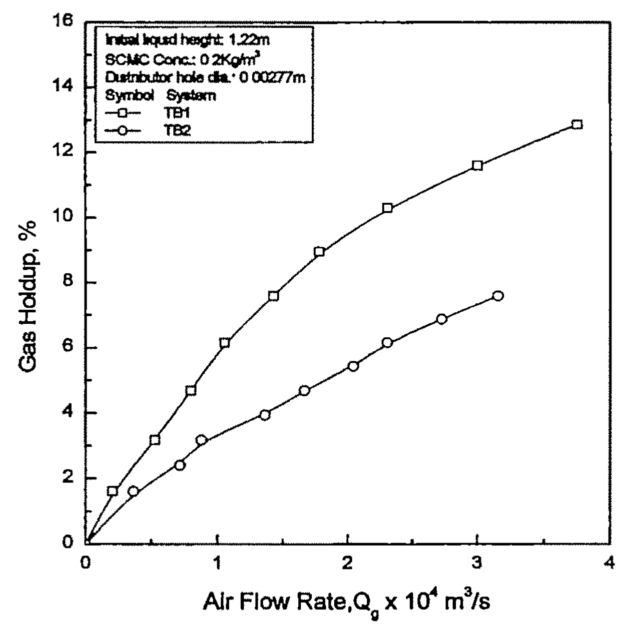

Fig. 3.9 Effect of the taper angle on holdup

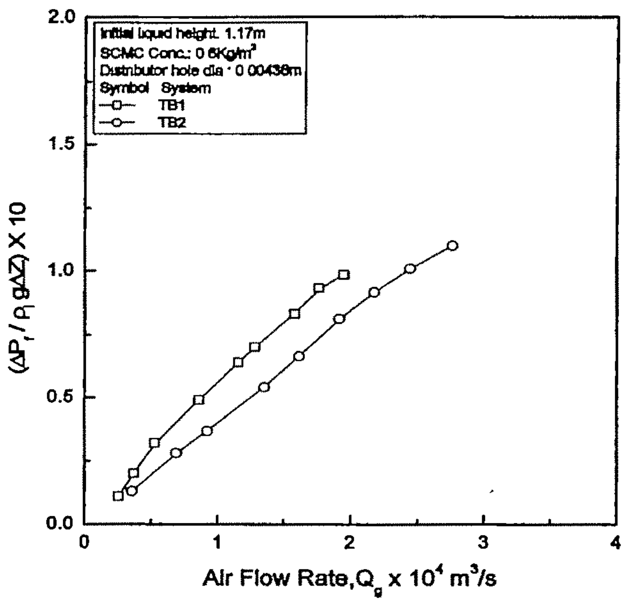

Fig. 3.10 Effect of the tapered angle on frictional pressure drop

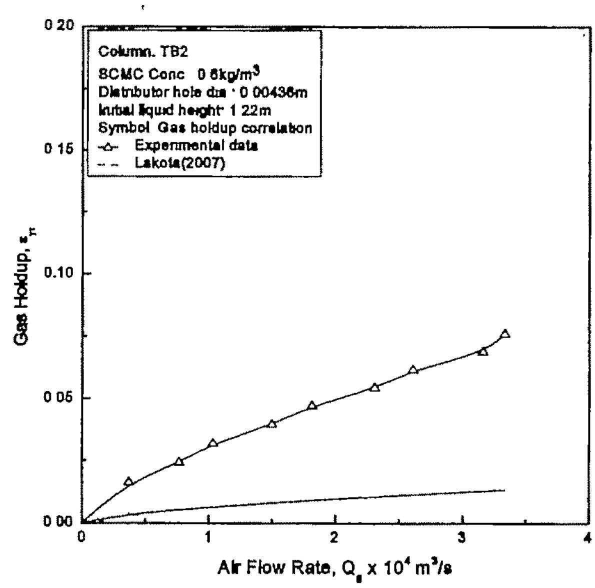

Fig. 3.11 Comparison of gas holdup data with well known correlation

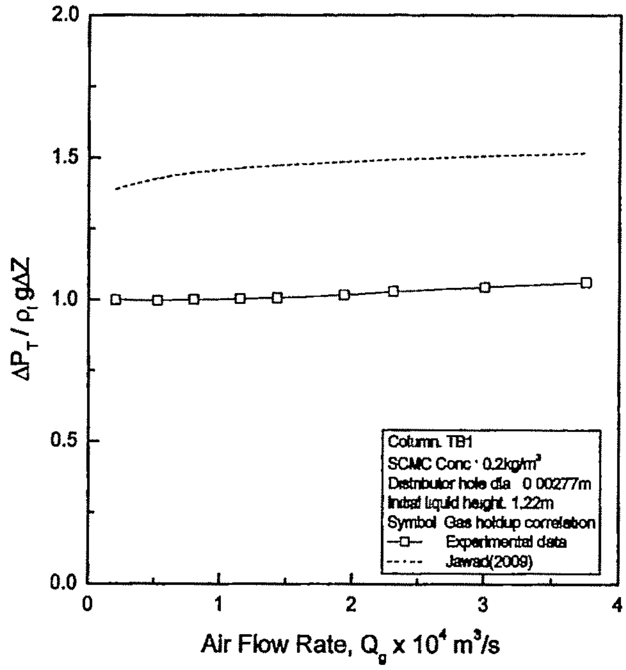

Fig. 3.12 Comparison of total pressure drop data with well known correlation

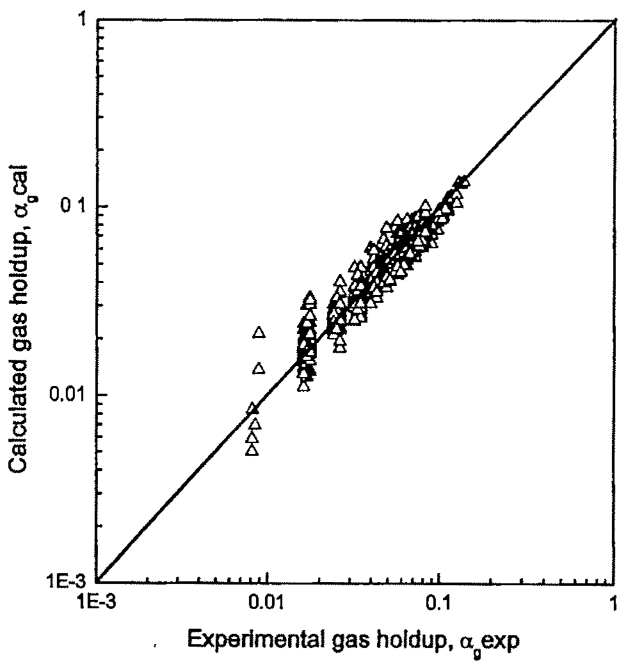

Fig. 3.13 Correlation plot of gas holdup

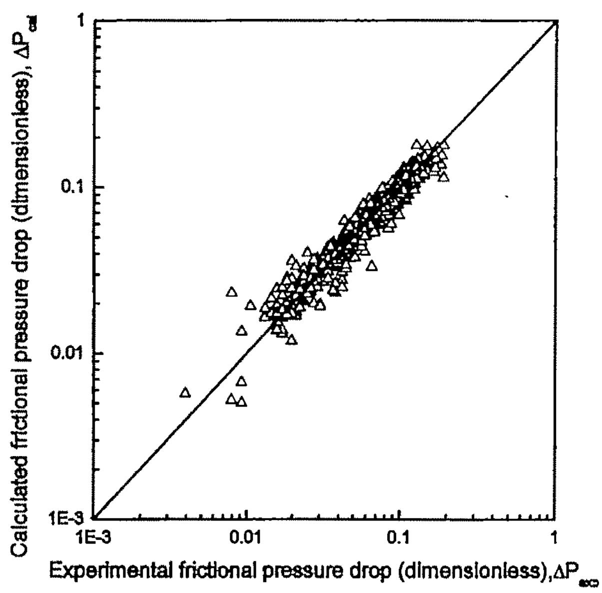

Fig. 3.14 Correlation plot of frictional pressure drop

Table 3.1 Comparison the holdup data with other correlation

Authors	RE (%)	AE
Godbole et al. (1982)	82.106	0.016
Vatai and Tekic (1987)	54.086	0.025
Fransolet et al. (2005)	59.863	0.024
Lakota (2007)	82.106	0.042
Eq. (3.25)	11.048	0.005

Table 3.2 Comparison total pressure drop data with other correlation

Authors	RE (%)	AE
Jawad (2009)	47.389	0.483
Eq. (3.29)	0.780	0.008